J. Fluid. Mech. (1986). *vol.* 165, *pp.* 355–372
Printed in Great Britain

A study of over-reflection in viscous Poiseuille flow

By RICHARD S. LINDZEN AND SANDRO RAMBALDI†
Massachusetts Institute of Technology, Center for Meteorology and Physical Oceanography, Cambridge, MA 02139, USA

(Received 28 December 1984 and in revised form 14 August 1985)

It is shown that viscous Poiseuille flow sustains wave propagation in its centre region for waves whose phase speed is less than the maximum flow speed. When, moreover, there are critical levels, there exists a range of phase speeds for which over-reflection occurs and this range corresponds exactly to the range for which unstable eigenmodes exist. Consistent with the conjecture of Lindzen & Barker (1985), it is found that viscous boundary layers around the critical level and at the wall replace the exponential regions and wave sinks required for inviscid over-reflection.

Over-reflection, we find is confined to phase speeds for which these two boundary layers are in close proximity rather than widely separated or substantially overlapping.

Over-reflection is inevitably associated with a wave phase tilt opposite in direction to the shear at the critical level. All other cases yield a phase tilt in the direction of the shear. The former is consistent with the condition for the Orr mechanism to produce amplification (Boyd 1983).

1. Introduction

In a recent analysis of wave over-reflection in plane parallel shear flow, Lindzen & Barker (1985; hereafter referred to as LB) determined what exactly was necessary in order to obtain such over-reflection. The question is an important one, since the existence of wave over-reflection (the reflection of waves where the reflection coefficient exceeds unity) is necessary in order to obtain normal mode instability in plane parallel shear flow (and in related problems with modest deviations from the plane-parallel constraint). Moreover, wave over-reflection is a more general property than is normal mode instability since only over-reflected waves satisfying very special quantization conditions become unstable normal modes, whereas over-reflection already indicates the ability of disturbances to extract energy from the basic state. Finally, LB suggested that over-reflection provided a unified approach to both viscous and inviscid stability problems – at least in those problems where away from boundaries and critical layers (where the real part of the disturbance phase speed equals the basic state flow speed), the inviscid equations are approximately applicable (i.e. at high Reynolds numbers). The purpose of this paper is to test this suggestion. Historically, viscous and inviscid instability have tended to be treated as different phenomena since it has long been known that viscous instability can exist for basic states which do not satisfy necessary conditions for inviscid instability. For unstratified shear flow, the classic example is Poiseuille flow which does not satisfy Rayleigh's Inflection Point Condition, but which is none the less unstable when viscosity is included.

† Permanent address: Department of Physics, University of Bologna, Italy.

Since LB is a very recent paper, it may prove helpful to review briefly those results in LB which are germane to the present study. First, it is important to explain what we mean by wave propagation. The equations for inviscid perturbations on basic shear flow can always be written in the form of a second-order Helmholtz equation with a clearly identifiable index of refraction for wave perturbations. Wave propagation requires that this index be positive and slowly varying (in a WKB sense). The existence of some such region in the flow is obviously essential for the existence of wave over-reflection. It is interesting to note, in this regard, that Couette flow does not have any such region (the index of refraction is always negative) and, indeed, Couette flow is always stable in a normal-mode sense regardless of whether viscosity is included or not. Poiseuille flow, on the other hand, does allow wave propagation.

Next, LB note that only waves having a critical level can be over-reflected. The critical level is the locus of energetic interaction between the wave and the mean flow. LB suggest that amplification at the critical level is by the Orr mechanism (Orr 1907; see Boyd 1983 for a particularly lucid explanation of this mechanism) which requires that at the critical level, the wave has a phase tilt which is opposite to that of the shear.

The simple existence of a critical level does not, by itself, lead to over-reflection. Usually the inviscid perturbation equation is singular at the critical level, and, if the critical level is in the propagation region, the wave's group velocity normal to the flow goes to zero at the critical level, suppressing the interaction. The point is that the travel time for a wave to reach the critical level goes to infinity. This can be overcome by interposing a turning point (where the index of refraction turns negative) between the wave region and the critical level. This allows the possibility of waves 'communicating' with the critical level at a finite rate since the group travel time remains finite up to the turning point, and tunnelling of wave flux in the 'exponential' region also proceeds at a finite rate.

LB finally note that such tunnelling of the wave flux will not occur unless there is a sink for the wave flux on the side of the critical level opposite the wave region. In an inviscid problem, this sink must be a second-wave propagation region (see Lindzen & Tung 1978, who show that the Rayleigh and Fjortoft conditions are equivalent to setting up the above configuration of propagation, tunnelling, and sink regions). However, LB have shown that for purposes of producing over-reflection, a region of concentrated wave damping (Rayleigh friction was used in LB) serves equally well as a sink. LB described the role of the sink as pulling the wave flux past the critical level. An equivalent, but more explicit, description is given in §4 of the present paper where we show that only when the sink is present does the phase of the wave at the critical level tilt in the direction required by the Orr mechanism. This phase tilt disappears in the absence of the sink or even when the sink is 'too' far from the critical level.

It was suggested in LB that the above situation was equally appropriate to a viscous fluid. The existence of a wave is still essential (hence, the stability of Couette flow and the instability of Poiseuille flow). However, the exponential region separating the wave region from the critical level and the second wave (sink) region on the opposite side the the critical level to the first (over-reflecting) wave region (both features being guaranteed by the Rayleigh and Fjortoft conditions) are no longer necessary. The role of the exponential region, it was suggested, could be played by the viscous boundary layer around the critical level. Similarly, it was suggested that the role of the wave flux sink could be played by the viscous boundary layer at a physical wall. Specific reference was made in LB to Poiseuille flow (a parabolic flow

in a bounded channel). As we have already mentioned, this flow is stable in the absence of viscosity (it lacks an inflection point), but is unstable when viscosity is included (Heisenberg 1924; Lin 1944). The main purpose of the present paper is to confirm the above suggestions. In doing so, we will be able to offer some simple insights into existing stability results.

In §2 we rederive the Orr–Sommerfeld equation for linear wave perturbations on Poiseuille flow primarily in order to establish our notation. We examine the wave character of solutions in the centre of the flow, evaluate the wave-group velocity, analyse the boundary layers at the critical level and at the boundary walls and obtain asymptotic expressions for the wave modes and viscous modes near the centre of the flow. We finally set up the mathematical problem of calculating the reflection coefficient for a wave sent from the centre of the flow toward a wall.

Section 3 describes our numerical algorithm for solving the above scattering problem. Resolution is discussed in the context of the above boundary-layer analysis. The algorithm is tested by using it to reproduce existing stability results for viscous Poiseuille flow (Grosch & Salwen 1968).

In §4 we discuss our results for wave over-reflection. We find that over-reflection (and instability) occurs only for a narrow range of critical levels where the critical-level boundary layer is in close proximity to the wall boundary layer or where the two boundary layers are slightly overlapping. The upper neutral stability curve of the classical Orr–Sommerfeld problem turns out to be associated with the former while the lower curve is associated with the latter (see Lin 1955, p. 38 for a description of the two branches; the present paper to the best of our knowledge, gives the first explanation of their existence). Both neutral curves are associated with unity wave reflection. The detailed amplitude and phase structure of over-reflected waves is examined and discussed in the light of the mechanism proposed by LB.

2. Governing equations and relevant properties

In this section we discuss the properties of the solution relevant to our numerical integration. We consider a Poiseuille flow, vanishing at the two sidewalls at $z = 0$, $2L$; the profile of the x-velocity is given by

$$U(z) = V\left(\frac{z}{L}\right)\left[2-\left(\frac{z}{L}\right)\right].$$

The linearized, non-dimensional perturbation equations are

$$\left.\begin{aligned}(\partial_t + U\partial_x)\,u' + w'\left(\frac{\mathrm{d}U}{\mathrm{d}z}\right) &= -\partial_x p' + \frac{\Delta u'}{Re},\\ (\partial_t + U\partial_x)\,w' &= -\partial_z p' + \frac{\Delta w'}{Re},\\ \partial_x u' + \partial_z w' &= 0,\end{aligned}\right\} \tag{2.1}$$

where the primes denote the non-dimensional perturbations, Re is the Reynold's number ($Re = VL/\nu$) and U is equal to $z(2-z)$. From (2.1) we eliminate the perturbation pressure, and we introduce a stream function ψ ($w' = -\partial_x \psi$ and $u' = \partial_z \psi$) to get the Orr–Sommerfeld equation

$$\left(\frac{\mathrm{d}^2 U}{\mathrm{d}z^2}\right)\partial_x \psi - (\partial_t + U\partial_x)\,\Delta\psi + \frac{\Delta^2 \psi}{Re} = 0. \tag{2.2}$$

Since the coefficients of (2.2) are independent of t and x, we look for a solution of the form

$$\psi(x, z, t) = \psi(z) \exp[ik(x-ct)], \tag{2.3}$$

and we get

$$\epsilon\frac{d^4\psi}{dz^4}+[(U-c)-2\epsilon k^2]\frac{d^2\psi}{dz^2}-\left[\frac{d^2U}{dz^2}+k^2(U-c)-\epsilon k^4\right]\psi = 0, \tag{2.4}$$

where $\epsilon = (i/kRe)$. In the inviscid case, (2.4) reduces to

$$\frac{d^2\psi}{dz^2}-\left[\frac{1}{U-c}\frac{d^2U}{dz^2}+k^2\right]\psi = 0,$$

and, for $k^2(1-c) < 2$, in the centre of the channel the solution is the superposition of a downward- and an upward-propagating wave. In the viscous case, for high Reynolds' number, the total solution is given by the superposition of these two wave modes, slightly modified by the presence of dissipation, and two viscous modes.

In order to numerically compute the reflection coefficient for a wave sent from the centre of the flow toward a wall, we must be able to identify in the total solution the upward and the downward propagating wave mode.

In order to identify the different modes in the middle of the flow, we consider a two-scale problem which takes into account the very high Reynolds number. Denoting the scale of variation of the solution by δ, and substituting $z = Z/\delta$, we get (from (2.4))

$$\epsilon\delta^4\frac{d^4\psi}{dZ^4}+\delta^2[B(z)-2\epsilon k^2]\frac{d^2\psi}{dZ^2}+[C(z)+\epsilon k^4]\psi = 0, \tag{2.5}$$

where ϵ is a small parameter. In the centre of the flow, $B(z) = (U-c)$ and $C(z) = [-(d^2U/dz^2)-k^2(U-c)]$ are order-one functions. Following the WKB technique (Bender & Orzag 1978) we write:

$$\left.\begin{aligned}
\psi(Z) &= \exp[D(Z)],\\
\dot\psi &= \dot D\psi,\\
\ddot\psi &= (\ddot D+\dot D^2)\,\psi,\\
\dddot\psi &= (\dddot D+3\dot D\,\ddot D+\dot D^3)\,\psi,\\
\ddddot\psi &= (\ddddot D+3\ddot D^2+4\dot D\,\dddot D+6\ddot D\,\dot D^2+\dot D^4)\,\psi,
\end{aligned}\right\} \tag{2.6}$$

where the dot stands for a derivative with respect to Z. We expand $D(Z)$ as a power series in of a new parameter Δ to be determined

$$D(Z) = \Delta^{-1}(E_0+\Delta E_1+\Delta^2E_2+\ldots). \tag{2.7}$$

Substituting (2.7) in (2.6) we get:

$$\begin{aligned}
\dot\psi &= \Delta^{-1}[\dot E_0+\Delta\dot E_1+O(\Delta^2)]\,\psi,\\
\ddot\psi &= \Delta^{-2}[\dot E_0^2+\Delta(2\dot E_0\,\dot E_1+\ddot E_0)+O(\Delta^2)]\,\psi,\\
\dddot\psi &= \Delta^{-3}[\dot E_0^3+\Delta(3\dot E_0^2\,\dot E_1+3\dot E_0\,\ddot E_0)+O(\Delta^2)]\,\psi,\\
\ddddot\psi &= \Delta^{-4}[\dot E_0^4+\Delta(4\dot E_0^3\,\dot E_1+6\dot E_0^2\,\ddot E_0)+O(\Delta^2)]\,\psi,
\end{aligned}$$

keeping only the leading terms and substituting into (2.5) we find:

$$\epsilon\left(\frac{\delta}{\Delta}\right)^4[\dot{E}_0^4+\Delta(4\dot{E}_0^3\dot{E}_1+6\dot{E}_0^2\ddot{E}_0)]+(B-2\epsilon k^2)\left(\frac{\delta}{\Delta}\right)^2[\dot{E}_0^2+\Delta(2\dot{E}_0\dot{E}_1+\ddot{E}_0)]+(C+\epsilon k^4)=0.$$

Looking at the dominant terms:

$$\epsilon\left(\frac{\delta}{\Delta}\right)^4\dot{E}_0^4+B\left(\frac{\delta}{\Delta}\right)^2\dot{E}_0^2+C=0,$$

and, taking into account that $|\epsilon|\ll 1$, we have only two consistent choices for $\Delta:\Delta=\delta$ and $|\epsilon|\,\delta^2=\Delta^2$.

For $\Delta=\delta$, we get the balance describing the two wave modes. From the zeroth- and first-order equation in Δ, we get

$$\dot{E}_0=\pm\mathrm{i}\left(\frac{C}{B}\right)^{\frac{1}{2}}, \tag{2.8a}$$

$$\dot{E}_1=\frac{-\ddot{E}_0}{(2\dot{E}_0)}\frac{-\epsilon(C/B+k^2)^2}{(2\Delta B\dot{E}_0)}, \tag{2.8b}$$

or, substituting back our original variable z,

$$\left(\frac{\mathrm{d}}{\mathrm{d}z}\right)D_\pm(z)=\pm\mathrm{i}\left(\frac{C}{B}\right)^{\frac{1}{2}}+\left(\frac{\mathrm{d}}{\mathrm{d}z}\right)\left[\ln\left(\frac{C}{B}\right)\right]^{-\frac{1}{4}}-\frac{(\pm k\,Re)^{-1}(C+k^2B)^2}{(2B^{\frac{1}{2}}C^{\frac{1}{2}})}. \tag{2.9}$$

The first term on the right-hand side of (2.9) is imaginary and describes only phase changes in the solution; the second term gives the wave amplitude variation due to the change in the index of refraction. Only the third term describes the effects of the dissipation, showing a small exponential growth or decay. This difference can be used to decide the sign of the energy flux (i.e. dissipating waves decay in the direction of propagation). Equation (2.9) describes the downward- and upward-propagating wave modes that in the next section will be noted by $F_1=\exp(D_-)$ and $F_2=\exp(D_+)$ respectively.

For $|\epsilon|\,\delta^2=\Delta^2$, we get the balance describing the two viscous modes. From the zeroth order in Δ, we find

$$\mathrm{i}\dot{E}_0^4+B\dot{E}_0^2=0,$$

giving four solutions for $\dot{E}_0$. Two are extensions of the wave modes ($\dot{E}_0^2=0$); the remaining two describe the viscous modes. Considering the zeroth- and first-order equation for the viscous modes we find:

$$\dot{E}_0=\pm(\mathrm{i}B)^{\frac{1}{2}}, \tag{2.10a}$$

$$\dot{E}_1=\frac{-5\ddot{E}_0}{(2\dot{E}_0)}+\frac{\epsilon(C+2k^2B)}{(2\Delta B\dot{E}_0)}, \tag{2.10b}$$

or, substituting back our original variable z,

$$\left(\frac{\mathrm{d}}{\mathrm{d}z}\right)D_\pm(z)=\pm(\mathrm{i}k\,Re\,B)^{\frac{1}{2}}+\left(\frac{\mathrm{d}}{\mathrm{d}z}\right)[\ln(B)]^{-\frac{5}{4}}\pm(\mathrm{i}k\,Re)^{-\frac{1}{2}}(C+2k^2B)\,(2B)^{-\frac{3}{2}} \tag{2.11}$$

Now the first term on the right-hand side of (2.11) is complex and proportional to ϵ^{-1} and these two solutions have strong exponential growth or decay respectively. We call these two solutions the viscous modes, and the mode that decays exponentially going from the centre of the flow toward the wall we call incident, implying that its source of energy must come from outside our domain. Equation (2.11) describes the

'incident and reflected' viscous modes that in the next section will be denoted by $F_3 = \exp(D_+)$ and $F_4 = \exp(D_-)$ respectively (taking $i^{\frac{1}{2}}$ in the first quadrant). Equations (2.9) and (2.11) contain all the information that we need to separate the four modes in the centre of the channel in our numerical calculations.

In the remainder of this section we briefly discuss the group velocity of the wave modes; this will be relevant for §5. We then discuss the thickness of the boundary layers present in our flow; this thickness is important because it determines the smallest scale that we must resolve in the numerical calculation.

2.1. *Group velocity*

We consider the inviscid form of (2.2) and we assume the scale of variation of U to be large compared with those of the solutions. Looking for a solution of the form

$$\tilde{\psi}(x, z, t) = \psi \exp[i(kx+mz-\omega t)],$$

we find the following local dispersion relation:

$$\omega = kU(z) - \frac{2k}{(k^2+m^2)}.$$

The component of the group velocity in the z-direction is then given by:

$$Cz_g = \left(\frac{\partial \omega}{\partial m}\right) = \frac{4km}{(k^2+m^2)^2}, \tag{2.12}$$

where $m^2 = -k^2+2/(U-c)$. We observe that Cz_g vanishes as we approach the critical level and its asymptotic behaviour, as U goes to c, is given by:

$$Cz_g \to (2)^{\frac{1}{2}} k(U-c)^{\frac{3}{2}}.$$

Note that $(Cz_g)^{-1}$ is not integrable as U approaches c.

2.2. *Boundary layers*

Using conventional boundary-layer analysis, it is easy to show that, at the walls, the following terms dominate (2.4):

$$\frac{d^4\psi}{dz^4}, \quad ik\,Re\,(U-c)\frac{d^2\psi}{dz^2},$$

leading to a boundary-layer scale $O(Re^{-\frac{1}{2}})$ or more precisely,

$$\delta_w = (kc\,Re)^{-\frac{1}{2}}.$$

Similarly at the critical level the following terms dominate:

$$\frac{d^4\psi}{dz^4}, \quad ik\,Re\frac{d^2U}{dz^2}\psi,$$

leading to a boundary-layer scale $O(Re^{-\frac{1}{4}})$ or more precisely,

$$\delta_c = \left|k\,Re\left(\frac{d^2U}{dz^2}\right)\right|^{-\frac{1}{4}}.$$

Note, that at high Reynolds number, δ_w tends to be much smaller than δ_c. Hence, if our numerical algorithm resolves the boundary layer at the wall, it will certainly be adequate to resolve the critical layers.

3. The numerical algorith: resolution and checks

Equation (2.4) has the form

$$\frac{\epsilon\,\mathrm{d}^4\psi}{\mathrm{d}z^4}+B(z)\frac{\mathrm{d}^2\psi}{\mathrm{d}z^2}+C(z)\,\psi=0 \tag{3.1}$$

where $B(z)$ and $C(z)$ now include the order-ϵ terms. In our numerical procedure we replace this fourth-order equation with a system of two second-order equations:

$$\left.\begin{aligned}\frac{\mathrm{d}^2\psi}{\mathrm{d}z^2}-\phi&=0,\\ \frac{\epsilon\,\mathrm{d}^2\phi}{\mathrm{d}z^2}+B\phi+C\psi&=0.\end{aligned}\right\} \tag{3.2}$$

Using the finite-difference representation of the second derivative, $\mathrm{d}^2f/\mathrm{d}z^2\simeq(f_{I+1}-2f_I+f_{I-1})/h^2$, we approximate (3.2) by

$$\boldsymbol{f}_{I-1}+\boldsymbol{M}_I\,\boldsymbol{f}_I+\boldsymbol{f}_{I+1}=0, \tag{3.3}$$

where $\boldsymbol{f}_I$ is a two-dimensional vector and $\boldsymbol{M}_I$ is a two-by-two matrix:

$$\boldsymbol{f}_I=\begin{vmatrix}\psi_I\\ \phi_I\end{vmatrix},\quad \boldsymbol{M}_I=\begin{vmatrix}-2 & -h^2\\ h^2C_I/\epsilon & (h^2B_I/\epsilon)-2\end{vmatrix}.$$

Equation (3.3) represents a banded tridiagonal system which we solve with the version of Gaussian elimination described by Lindzen & Kuo (1969). Briefly, we define a matrix $\boldsymbol{E}_I$ and a vector $\boldsymbol{g}_I$ such that

$$\boldsymbol{f}_I=\boldsymbol{E}_I\boldsymbol{f}_{I+1}+\boldsymbol{g}_I. \tag{3.4}$$

Substituting (3.4) into (3.3.) we find

$$\boldsymbol{E}_I=-(\boldsymbol{E}_{I-1}+\boldsymbol{M}_I)^{-1},\quad \boldsymbol{g}_I=\boldsymbol{E}_I\,\boldsymbol{g}_{I-1}. \tag{3.5a}$$

To compute the solution of (3.3.) we proceed in two steps. First, using (3.5a), we compute $\boldsymbol{E}_I$ and $\boldsymbol{g}_I$ (all $\boldsymbol{g}_I$ vanish) starting from the wall and proceeding toward the centre of the flow. At the wall we use the boundary conditions $u'=v'=0$; in the finite-difference approximation this gives $\psi_1=0$ and $\phi_1=(2/h^2)\,\psi_2$, which in turn imply

$$\boldsymbol{g}_1=\begin{vmatrix}0\\ 0\end{vmatrix},\quad \boldsymbol{E}_1=\begin{vmatrix}0 & 0\\ 2/h^2 & 0\end{vmatrix}. \tag{3.5b}$$

Equation (3.5b) allows us to use (3.5a) to calculate all the $\boldsymbol{E}_I$s and $\boldsymbol{g}_I$s. To complete the solution (i.e. to determine the $\boldsymbol{f}_I$s using (3.4)) we need boundary condition at the centre of the flow. This will, in fact, turn out to be our scattering relation.

In order to obtain the 'centre' boundary condition, we formally write our solution in terms of the four modes discussed in §2:

$$\psi(z)=IF_1(z)+RF_2(z)+I_{\mathrm{v}}\,F_3(z)+R_{\mathrm{v}}\,F_4(z), \tag{3.6}$$

where I (incident) and R (reflected) denote the amplitudes of the 'inviscid' modes propagating energy toward and away from the wall respectively, while I_{v} (incident viscous) and R_{v} (reflected viscous) denote the amplitude of the two viscous modes. We call incident (reflected) the viscous mode whose amplitude, due to the presence of dissipation, decreases (increases) as we approach the wall. The functions F_1, F_2, F_3,

F_4 have been evaluated in §2 ((2.8) and (2.10)). We do not want any incident viscous mode; we want to specify the incident wave mode and we want to compute the reflected wave mode and the reflected viscous mode. Therefore our boundary condition becomes

$$I = 1 \quad I_v = 0 \tag{3.7}$$

at the centre of the flow.

To apply these boundary conditions we write the first derivative of the solution in finite-difference form as:

$$\frac{\mathrm{d}\boldsymbol{f}_{IM}}{\mathrm{d}z} = [(\boldsymbol{E}_{IM}{}^{-1} - \boldsymbol{E}_{IM-1})/(2h)]\boldsymbol{f}_{IM} = U\boldsymbol{f}_{IM},$$

where the subscript IM denotes the point at the centre of the flow. Then, using (3.6) and (3.7) we write the solution as:

$$\boldsymbol{f}_{IM} = \boldsymbol{S}_{IM}\boldsymbol{r} + \boldsymbol{t}_{IM} \quad (\mathrm{d}/\mathrm{d}z)\boldsymbol{f}_{IM} = (\mathrm{d}\boldsymbol{S}_{IM}/\mathrm{d}z)\,\boldsymbol{r} + (\mathrm{d}/\mathrm{d}z)\,\boldsymbol{t}_{IM},$$

where

$$\boldsymbol{S} = \begin{vmatrix} F_2 & F_4 \\ (\mathrm{d}^2/\mathrm{d}z^2)\,F_2 & (\mathrm{d}^2/\mathrm{d}z^2)\,F_4 \end{vmatrix}, \quad \boldsymbol{r} = \begin{vmatrix} R \\ R_v \end{vmatrix}, \quad \boldsymbol{t} = \begin{vmatrix} F_1 \\ (\mathrm{d}^2/\mathrm{d}z^2)\,F_1 \end{vmatrix},$$

and we find:

$$\boldsymbol{r} = [(\mathrm{d}\boldsymbol{S}_{IM}/\mathrm{d}z) - U\boldsymbol{S}_{IM}]^{-1}[U\boldsymbol{t}_{IM} - (\mathrm{d}\boldsymbol{t}_{IM}/\mathrm{d}z)],$$

and

$$\boldsymbol{f}_{IM} = \boldsymbol{S}_{IM}[(\mathrm{d}\boldsymbol{S}_{IM}/\mathrm{d}z) - U\boldsymbol{S}_{IM}]^{-1}[U\boldsymbol{t}_{IM} - (\mathrm{d}\boldsymbol{t}_{IM}/\mathrm{d}z)] + \boldsymbol{t}_{IM}.$$

If we are only interested in the reflected waves R, we do not need to go back to (3.4) and compute the solution $\boldsymbol{f}_I$, therefore we do not need to save $\boldsymbol{E}_I$ and the full computation can be done with only a few dozen memory locations independent of the resolution. The full algorithm proved to be numerically stable even when using several thousand points. All computations presented here were done using 800 points from the centre of the flow to the wall; this value was chosen so that there would be only a small error both from the finite difference approximation and the truncation error introduced by the computer in single precision. We also verify that this resolution was sufficient to solve the boundary layer at the wall the scale of which (see §2) is much smaller than that of the boundary later at the critical level. Typical values ($k = 1$, $R = 10000$) give $\delta_w = 0.01$ and $\delta_c = 0.08$.

In order to check our numerics we compute the eigenvalue and the eigenfunction of the first even unstable eigenmode of the A family at $k = 1$ and $R = 10000$. We then compare our results with the results of Thomas (1953) (as referred to in Grosch & Salwen 1968). We find full agreement with his value of $c = 0.2375 + 0.0037\mathrm{i}$ (an eigenmode of the Poiseuille can be found with our technique, looking, in the complex plane, for the value of c such that the amplitude and the phase of the reflected wave coincides with those of the incident wave).

4. Results for wave over-reflection

Since the results we present are primarily illustrative, we will confine ourselves to a single Reynolds' number $Re = 10000$. As we see from figure 1, there are unstable normal modes for $0.8 < k < 1.13$ with the real part of the phase speed, c_r, ranging from 0.21 (lower neutral branch) to 0.25 (upper neutral branch). Note that Grosch

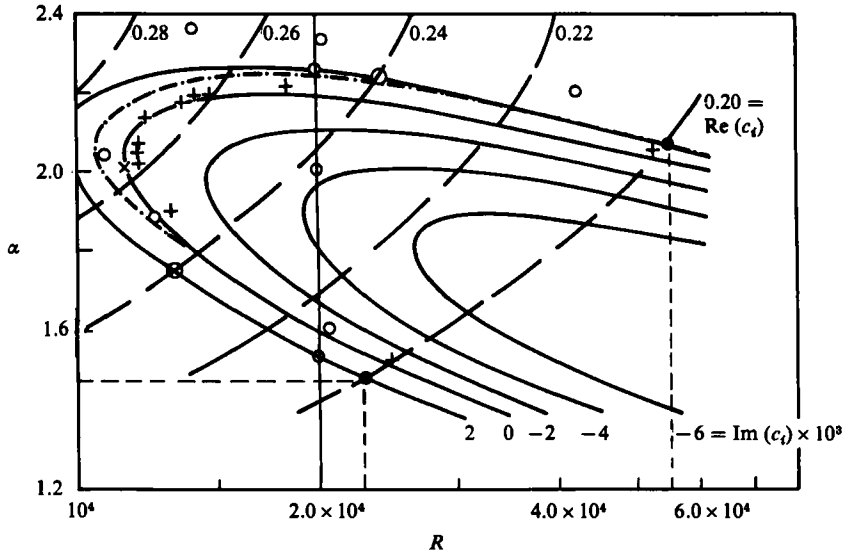

FIGURE 1. Curves of constant amplification, Im (c) = constant (solid line). Curves of constant phase velocity, Real (c) = constant (dashed line). From Grosch & Salwen 1968.

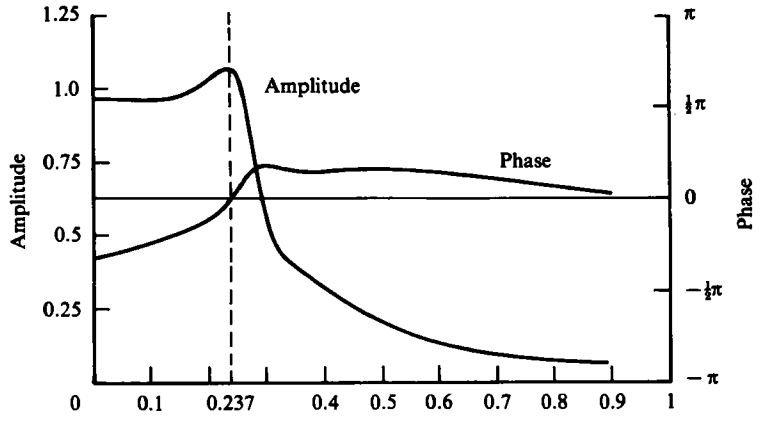

FIGURE 2. Amplitude and phase of reflection coefficient as function of the phase speed, c, for $k = 1$ and $Re = 10000$.

& Salwen's α is twice our k and their definition of Re is twice ours. Our qualitative results are essentially the same for any choice of Re (we explored $5000 < Re < 40000$).

In figure 2 we show the magnitude of the reflection coefficient, $|R|$, evaluated in the centre of the parabolic flow (as described in §3) as a function of c_r for $k = 1$. We see that over-reflection occurs only in a narrow region around the value of c_r for which unstable normal modes exist. In figure 3 (a–d) we show the relative magnitudes of terms 1, 2 and 3 (the first, second and third terms) in (2.2) for $k = 1$ and $c_r = 0.1$, 0.237, 0.4 and 0.8 respectively. Our convention in these figures is to scale the dominant term at any point to 1 and show the relative magnitudes of the remaining two terms. For $c_r = 0.8$ and 0.4, we see that inviscid regimes (characterized by a balance between terms 1 and 2), critical layers (balance between terms 1 and 3), and wall boundary layers (balance between terms 2 and 3) are well separated. For

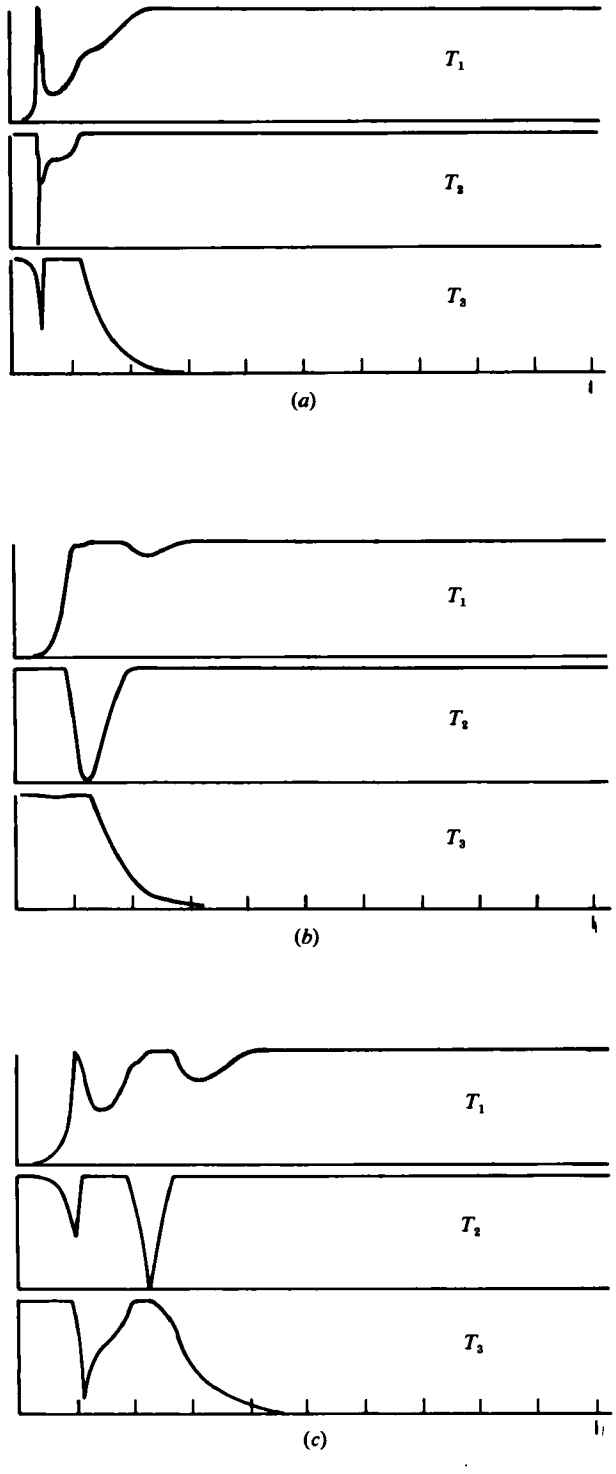

FIGURE 3 (*a*, *b*, *c*). For caption see facing page.

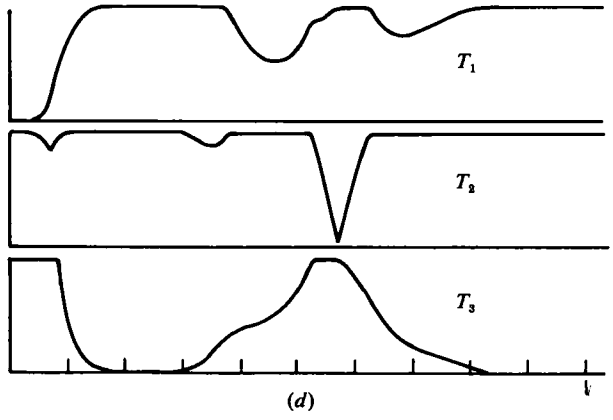

FIGURE 3. Relative amplitudes of the three terms in (2.2) for $k = 1$ and (*a*) $c_r = 0.1$; (*b*) $(c)_r = 0.237$; (*c*) $c_r = 0.4$; (*d*) $c_r = 0.8$, $Re = 10000$ for all cases.

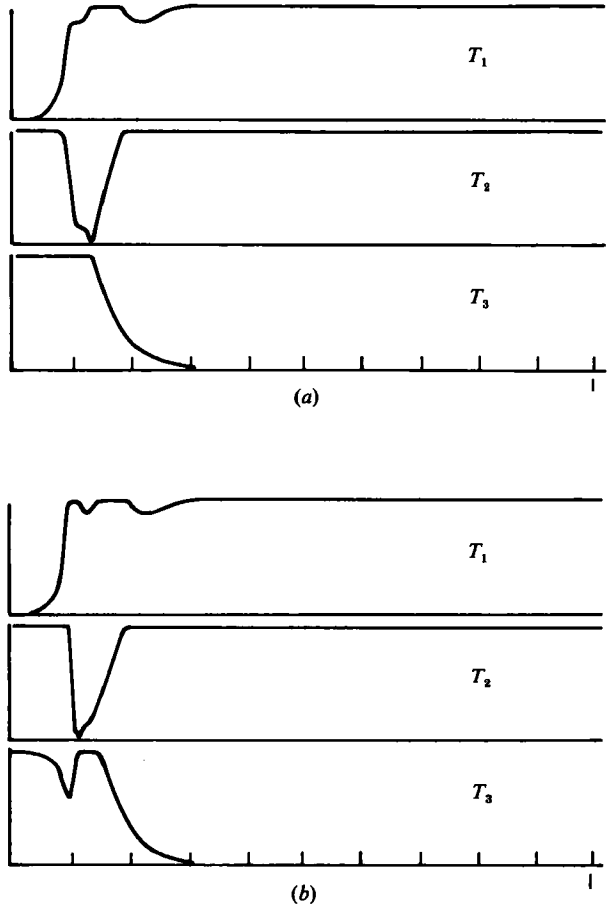

FIGURE 4. Same as figure 3 but (*a*) for $k = 0.0931$ and $c_r = 0.2463$ and (*b*) for $k = 0.797$ and $c_r = 0.2124$. These correspond to upper and lower neutral modes.

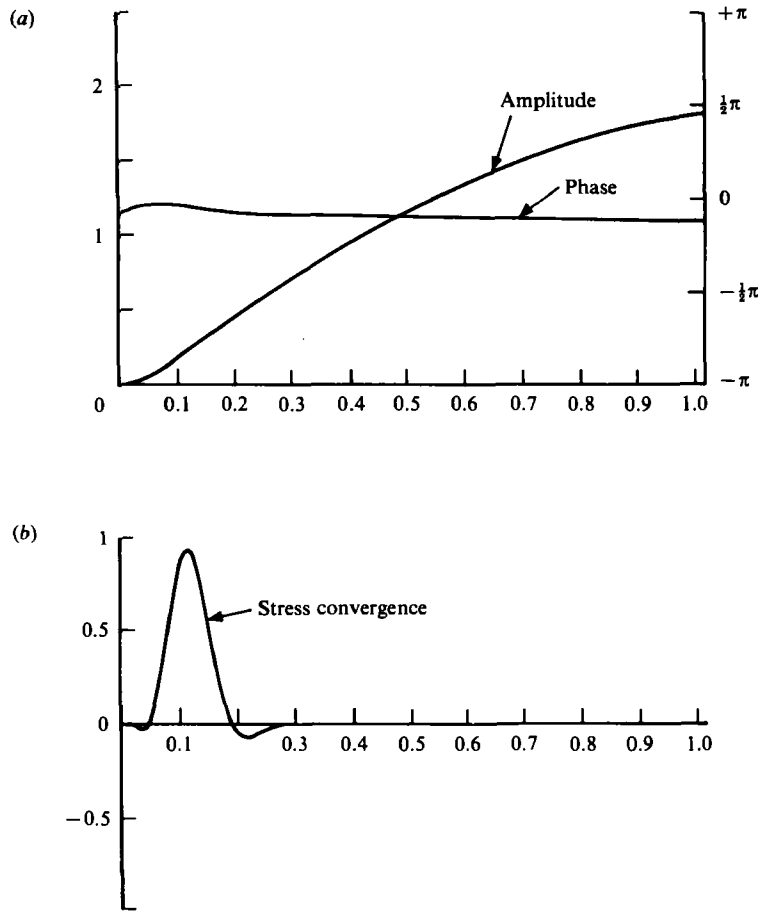

FIGURE 5. (*a*) Amplitude and phase of incidental plus reflected wave (i.e. total wave field) *vs.* *z*. (*b*) Convergence of Reynolds stress *vs* *z*. ($k = 1$; $c_r = 0.1$; $Re = 10000$.)

$c = 0.237$ (maximum over-reflection), the two layers are essentially touching.† For $c = 0.1$ the critical layer is embedded in the boundary layer and barely identifiable.

Reference to figures 7 and 8 shows that when the critical layer and the boundary layer are well separated the critical layer absorbs incident waves almost exactly as it would in the absence of the wall boundary layer; for $c = 0.1$ (see figure 5), the wave essentially only sees a slightly absorbing reflecting wall as though there were no critical layer. Only when the two layers are close or slightly overlapping does over-reflection occur.

In figure 4(*a*, *b*) we show the same quantities as in figure 3, but now for different values of k, $k = 0.797$ and $c_r = 0.2124$ (lower neutral point of figure 1) and $k = 1.093$ and $c_r = 0.2453$ (upper neutral point). These two points correspond to neutral normal modes where $R = 1$. For the lower neutral point the critical layer and the boundary

† Note that the boundary layers in figure 3(*a–d*) do not necessarily have *extents* equal to the boundary-layer *scales* derived in §2. This is particularly true for the wall boundary layer. An examination of the solution in the wall boundary layer confirms that the fields there vary on the boundary-layer scale, but that the boundary layer (defined by the balance of the second and third terms in 2.2) extends for several boundary-layer scales.

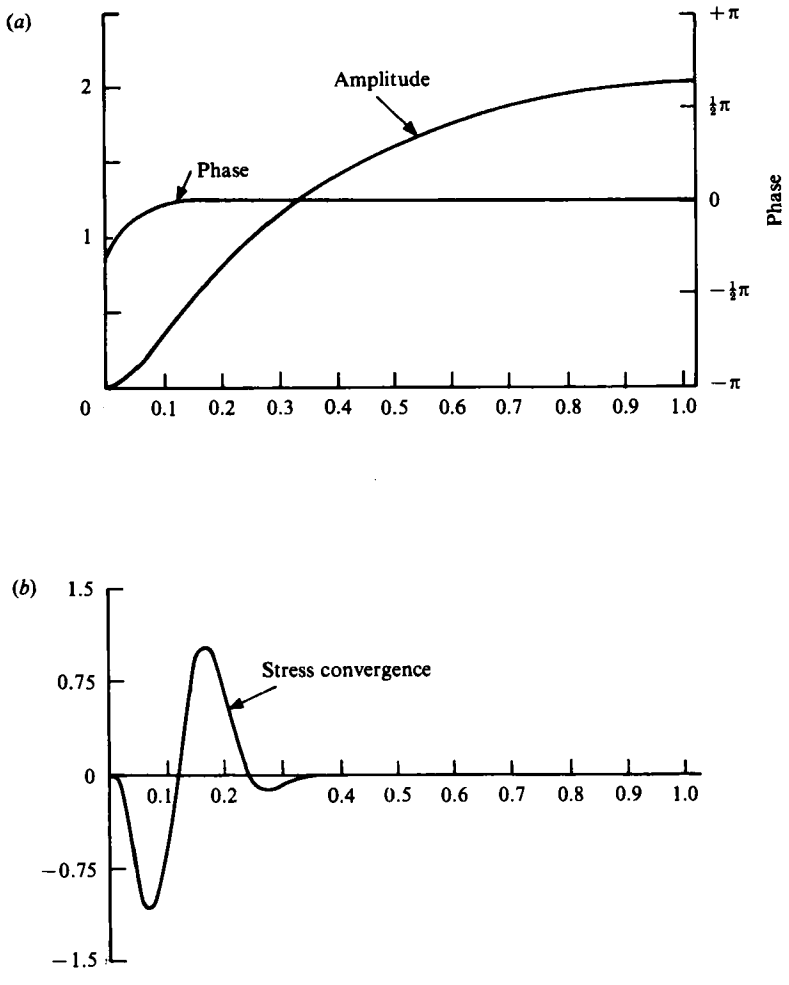

FIGURE 6. Same as figure 5 but for $k = 1$ and $c_r = 0.2375$.

layer are still distinguishable – but very close, and for the upper neutral point the two layers are slightly overlapping.

A better understanding of what is going on is given by the upper panels of figures 5–10 for the above values of c_r and k. The figures show the amplitude and phase of the total solution (incident plus reflected waves). When the layers are well separated, we have mostly just the incident wave, and its phase tilt is in the direction of the shear so that the Orr mechanism does not operate (or rather acts only to cause decay of perturbation energy). To be sure, the boundary layer produces a tilt in the direction appropriate to Orr magnification. However, the boundary layer is far removed from the critical layer and wave amplitudes at the boundary layer are very small. However, when the two layers are next to each other (figures 3*b*, 6), the appropriate tilt occurs within the critical layer allowing the Orr mechanism to operate. The situation disappears when the critical layer is embedded in the boundary layer (figures 3*a*, 5); presumably the Orr mechanism is swamped by damping. The lower panels of figures 5–10 show the Reynolds stress convergence associated with the above cases. Positive convergence is associated with wave absorption. In figure 5 we essentially have only

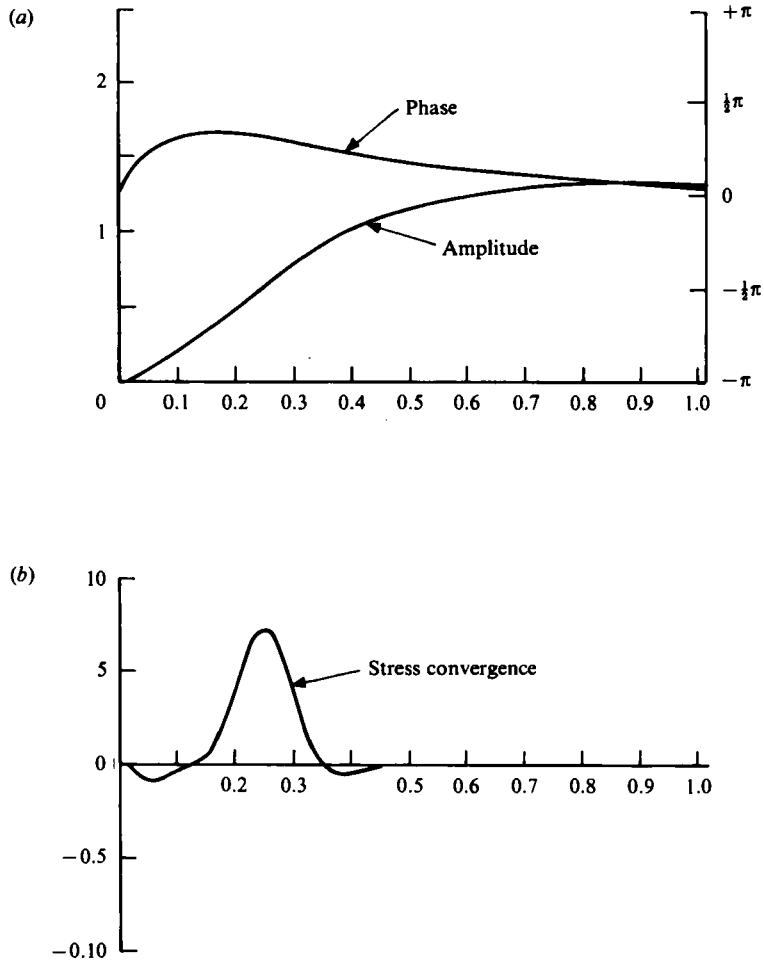

FIGURE 7. Same as figure 5 but for $k = 1$ and $c_r = 0.4$.

wave absorption by the boundary layer and in figures 7 and 8 only wave absorption by the critical layer. However in figures 9 and 10 we have Reynolds stress divergence which balances convergence and in figure 6 the divergence exceeds the convergence leading to over-reflection.

5. Estimates of growth rate from wave over-reflection

As we can see from figure 2, for $k = 1$ and Reynolds' number $Re = 10000$, we have over-reflection for a narrow region around $c = 0.237$ (the reflection coefficient R is 1.042 at $c = 0.237$). In the same region the phase of the reflected wave crosses zero suggesting the presence of a nearby (in the complex plane) unstable eigenmode for which we find $c = 0.2375 + 0.0037\mathrm{i}$.

We would like to relate the growth rate of this eigenmode with the increase of wave energy due to the over-reflection and the travel time of the energy from the centre

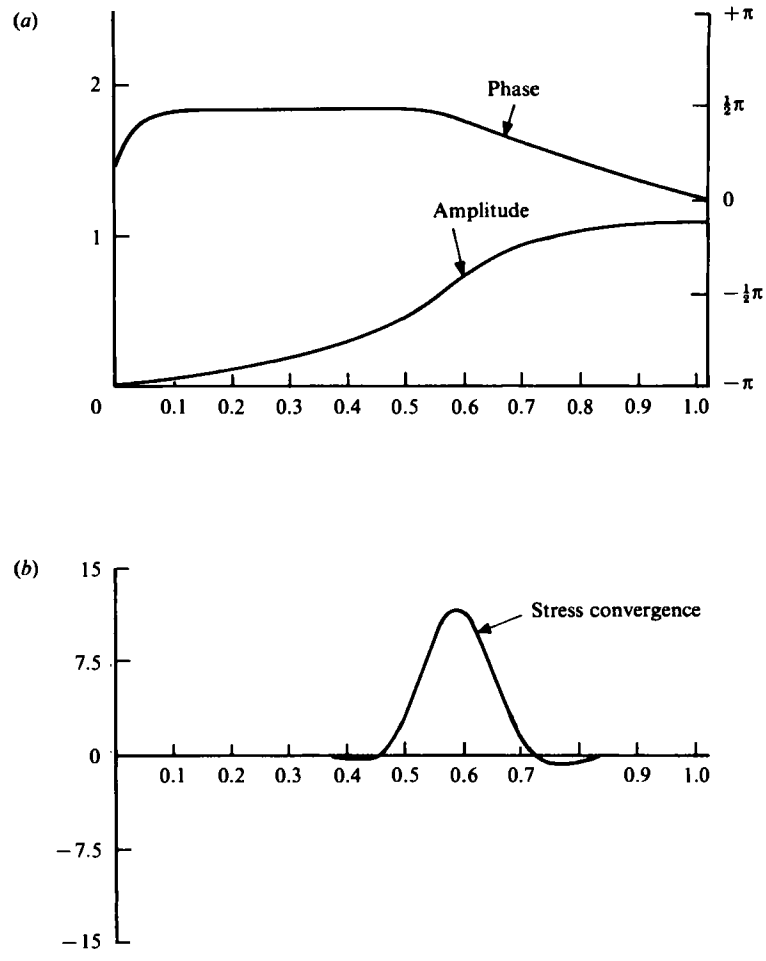

FIGURE 8. Same as figure 5 but for $k = 1$ and $c_r = 0.8$.

of the flow to the critical level and back to the centre of the flow. In particular we would like to verify the following expression:

$$\exp(\sigma T) = R, \tag{5.1}$$

where σ is the growth rate, T is the travel time from one over-reflecting critical layer to the other (recall that there are two over-reflecting critical layers in a parabolic flow – one on each side of the centre) and R is the reflection coefficient. If we substitute the values of the previous paragraph we compute $T = 11.12$ (in our non-dimensional units). Because the energy travels with the group velocity, which expression was given in §2, we can compute the travel time to go from $-Z$ to $+Z$ using:

$$T(Z) = 2\int_0^Z (Cz_g)^{-1}\,\mathrm{d}z, \tag{5.2}$$

but this expression diverges as Z approaches a critical level (also the WKB analysis breaks down). We can compute, using (5.2), the distance travelled in a time $T = 11.12$ and we find $z = 0.140$, a distance of 0.013 from the critical level (in this computation

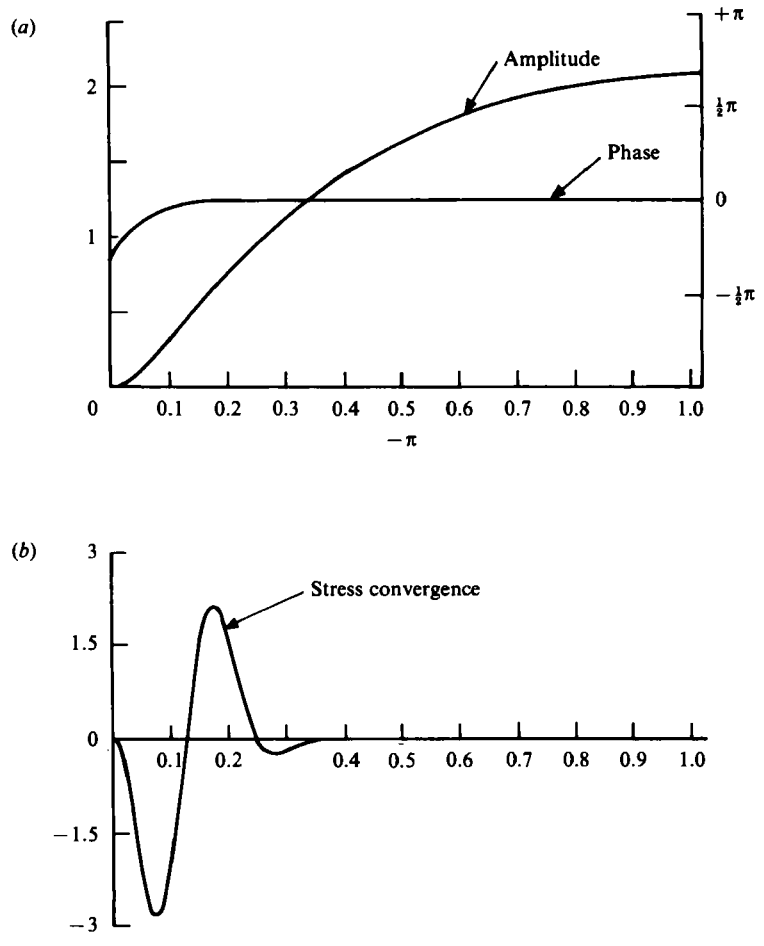

FIGURE 9. Same as figure 5 but for $k = 1.093$ and $c_r = 0.2463$.

$z_c = 0.127$). These results are shown in figure 11. (To compute $T(z)$ we remove its singularity adding and subtracting the singular analytically integrable function $G(z)$ given by:

$$G(z) = \frac{2^{-\frac{1}{2}}k^{-1}}{(\mathrm{d}U/\mathrm{d}z)^{\frac{5}{2}}}\left((z-z_c)^{-\frac{3}{2}} + \left(\frac{(\mathrm{d}u/\mathrm{d}z)}{4k^{-2}} + \frac{1.5}{(\mathrm{d}U/\mathrm{d}z)}\right)(z-z_c)^{-\frac{1}{2}}\right),$$

where $(\mathrm{d}U/\mathrm{d}z)$ is computed at $z = z_c$.)

Note that for the above to be useful, one would have to be able to identify the above value of z a priori. Reference to figure 3(*b*) shows that z lies, not implausibly, about half way between z_c and that value of z where the second and third terms in (2.2) are equal. However, this relation has not been proven; nor has it been tested at length.

6. Concluding remarks

We have shown that wave over-reflection is as appropriate to the understanding of viscous shear instability as it is to the inviscid problem. The concept allows us to

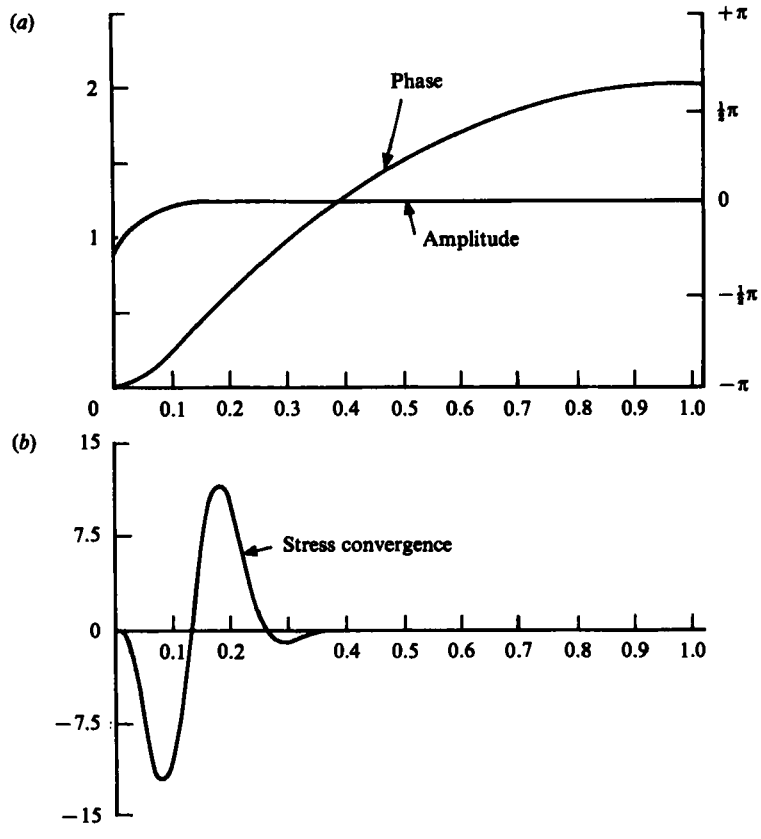

FIGURE 10. Same as figure 5 but for $k = 0.797$ and $c_r = 0.2124$.

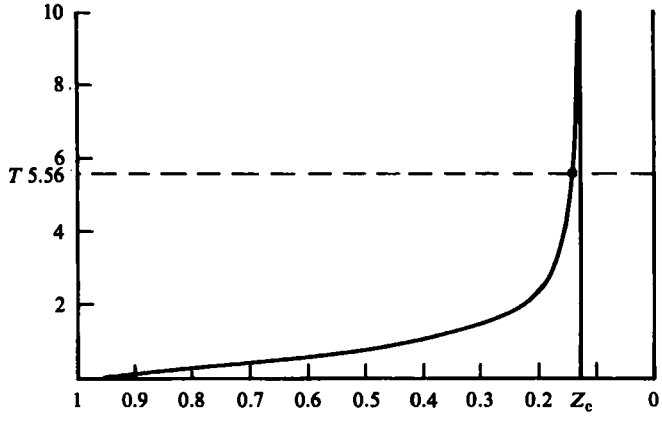

FIGURE 11. Half the travel time *vs.* distance from centre of jet. See text for details.

conveniently understand why viscous Poiseuille flow is unstable while viscous Couette flow is not. The point is simply, that at sufficiently high Reynolds numbers Poiseuille flow permits propagating vorticity waves while Couette flow does not. As with the inviscid stability problem, inviscid Poiseuille flow does not satisfy the necessary (and in the case of over-reflection, sufficient) conditions for over-reflection derived by Lindzen & Tung (1978). However, consistent with the conjecture of LB we find that

the missing components of the wave over-reflection geometry (a tunnelling region in front of the critical level and a wave sink in back of the critical level) can be simulated by viscous boundary layers. In contrast, to the inviscid problem where the wave sink is automatically adjacent to the critical level, the wave sink (i.e. the boundary layer at the wall) and the critical level are arbitrarily separable in the viscous problem. We find that over-reflection occurs only when the wall boundary layer and the critical-level boundary layer are close or slightly overlapping. This provides a convenient explanation of why instability exists for only a narrow range of phase speeds.

This work was supported by National Science Foundation under Grant ATM-82-05638 and NASA under Grant NGL 22-007-228 and NAGW-578, both at M.I.T.

REFERENCES

BENDER, C. M. & ORZAG, S. A. 1978 *Advanced Mathematical Methods for Scientists and Engineers.* McGraw Hill.

BOYD, J. P. 1983 *J. Atmos. Sci.* **40**, 2304.

GROSCH, C. E. & SALWEN, H. 1968 *J. Fluid. Mech.* **34**, 177.

HEISENBERG, W. 1924 *Ann. Phys., Lpz.* (4), **74**, 577.

LIN, C. C. 1944 *Proc. Nat. Acad. Sci.* **30**, 316.

LIN, C. C. 1955 *The Theory of Hydrodynamic Stability.* Cambridge University Press.

LINDZEN, R. S. & BARKER, J. W. 1985 *J. Fluid. Mech.* **151**, 189.

LINDZEN, R. S. & KUO, A. L. 1969 *Mon. Wea. Rev.* **97**, 732.

LINDZEN, R. S. & TUNG, K. K. 1978 *J. Atmos. Sci.* **35**, 1626.

ORR, W. McF. 1907 *Proc. R. Irish Acad.* **27**, 9.

THOMAS, L. H. 1953 *Phys. Rev.* (2), **91**, 780.